

Report

Project Title: Implantable 3D-Printed Plant Sensors: Continuous Assessment of Nutrient Measurements in Corn Fields.

PI: Azahar Ali, School of Animal Sciences, Virginia Tech (azahar@vt.edu)

Co-PI: Dong Ha, ECE department, Virginia Tech, dha@vt.edu

Report till Dec 2024: In this proposal, two objectives were outlined: the development of plant-implantable sensors during the first year and corn field trials for sensor validation in the second year (refer to the table below for each task). To complete our **Objective #1** of the proposal, we have successfully developed the plant implantable sensors for measuring nitrogen (N), phosphorus (P), and potassium (K) uptake in corn plants and calibrated the sensors.

Objective 1: Manufacturing of low-cost, field-deployable and implantable sensors using 3D nano-printing for continuous monitoring of nitrate (NO_3^- or N), and phosphate (PO_4^{2-} or P) uptake in corn plants. The needle-type implantable sensor allows direct insertion into the corn plant for *in situ* measurement of these nutrients under different fertilizer environments. Sensors will be interfaced with wireless sensor nodes for data collection remotely.

Proposed tasks in this project	Year 1	Year 2
Development of plant implantable sensors and calibration: Sensor manufacturing, sensor calibration, wireless circuit development, sensor calibration, and filing patent		
Corn field trials and validation: Design the experiment with corn fields (Kentland farm), corn stalk sample collection from corn fields with fertilizer treatments, analysis of stalk samples, deploy sensors, data analysis and yield studies		

Sensor Manufacturing: As objective 1, we have successfully manufactured a needle-shaped, plant-implantable sensor (Figure 1). This sensor is equipped with three detection units for monitoring N, P, and K nutrients and features an insertable design for integration into the corn plant stalk. Figure 1 also illustrates how the sensor can be connected to a readout circuit to collect sensing data. This low-cost, plant-implantable sensor is fabricated using a 3D printing method known as stereolithography (SLA)-based extrusion printing, following the sensor design shown in Figure 1. Utilizing the SLA method, we employed a high-temperature polymer resin to create the sensor base. The process involves two steps—printing and curing—and allows for the simultaneous production of up to 20 sensors. After curing, the sensor is covered with a shadow mask for selective deposition of a thick gold layer (300 nm) using a DC sputtering technique. Each sensor incorporates three detectors for N, P, and K nutrients and one shared reference electrode (RE). The reference electrode is further modified with silver/silver chloride ink and a solid electrolyte to mitigate chloride leaching over the measurement period. To enable sensor calibration, each

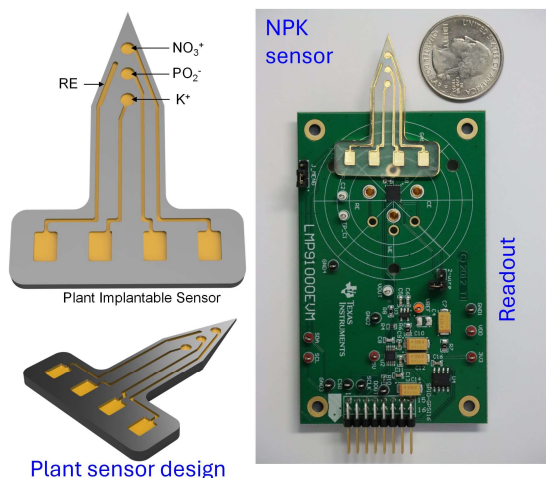


Figure 1. Manufactured implantable needle-based plant sensor for NPK monitoring in corn plants.

detector was modified with a specific ion-selective membrane tailored to the corresponding nutrient. The specific ion-selective membrane (ISM) was to improve the selectivity of the measurement as plant water is a complex matrix. See our recently published papers as references for nitrate and phosphate detection with improve selectivity.^{1,2}

Sensor calibration: We have successfully calibrated the needle-based plant sensor and analyzed the results by applying machine learning algorithms. Preliminary results of this proposal are shown in Figs 2–4.

K–sensor: The results of potassium (K) sensing are shown in **Fig. 2**. One of the electrodes in our plant implantable sensor (shown in **Fig. 1**) was modified with *K*-ISM layer so that this detector can detect only K ions in a test media. During testing, we introduced a number of dose-dependent potassium concentrations and recorded the K–sensor’s open circuit potential (OCP). The open circuit potential of the K-sensor is directly proportional to the K^+ concentrations. This behavior is attributed to the potassium ion-selective membrane (*K*-ISM), which traps K^+ ions from the testing solution, generating an interfacial potential that alters the overall OCP of the sensor (**Fig. 2A**). As tested, this K–sensor can detect a very low concentration of K^+ ion, which is 10 ppb and can detect a higher concentration of 200 ppm. The ability to detect 10 ppb of K^+ ions is primarily attributed to the sensor's wrinkled surface structure.¹ This K–sensor showed a high selectivity as evidenced by its low relative standard deviation of ± 7.8 (**Fig. 2C**).

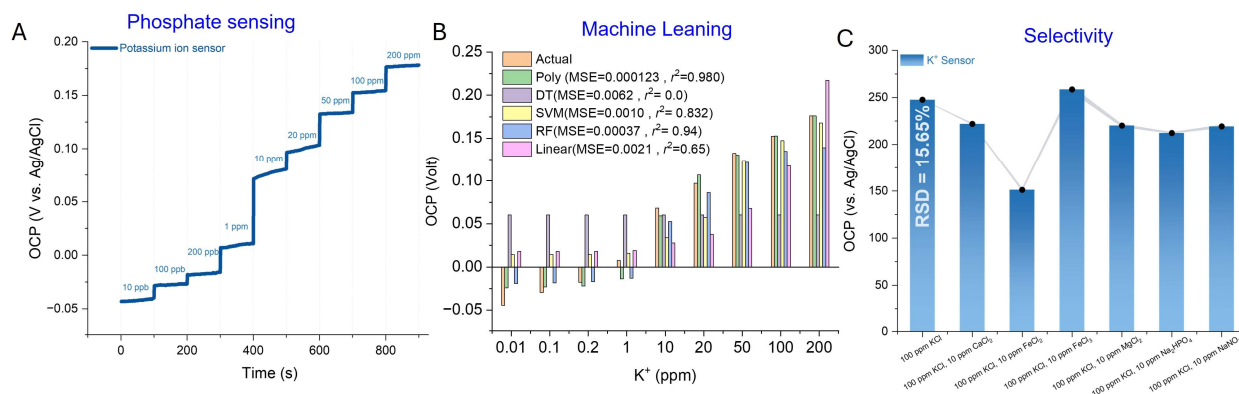


Figure 2. A) Calibration plot of the K-sensor, demonstrating its performance over a wide range of potassium ion concentrations (10 ppm to 200 ppm). B) Machine learning analysis using various regression models to determine the best fit for the calibration graph. C) Selectivity studies highlighting the sensor's response in the presence of common interfering ions.

To analysis the sensor data, we employed supervised machine learning³⁻⁵ to predict our NPK plant sensor’s output as plant tissue and physiological fluid are complex matrices.⁶ Decision Tree regression was used for its ability to capture non-linear relationships and complex patterns by splitting the data into segments. Support Vector Machine (SVM) Regression was chosen due to its strength in modeling non-linear relationships and its robustness in high-dimensional spaces. Polynomial Regression was applied to model potential curvilinear relationships by introducing higher-degree terms, allowing for more flexibility than linear regression. Random Forest Regression was used for its ability to handle complex datasets by combining multiple decision trees, improving robustness and reducing overfitting. Lastly, Linear Regression served as a baseline, offering a simple and interpretable model for situations where the relationship between concentration and sensor output is approximately linear. These models were selected to comprehensively assess both linear and non-linear relationships in the data, ensuring the best model for predicting plant sensor outputs based on their respective concentrations. In **Fig. 2B**, the results show that

Polynomial Regression outperforms all other models with the highest r^2 (0.9803) and the lowest MSE (0.0001233), making it the best fit for predicting potassium concentration. Random Forest Regression follows closely with an r^2 of 0.9405 and MSE of 0.0003723, offering strong accuracy. SVM Regression also performs well with an r^2 of 0.8322 and MSE of 0.0010503. Linear Regression provides a weaker fit ($r^2 = 0.6491$, MSE = 0.0021965), and Decision Tree Regression performs poorly, with r^2 of 0 and MSE of 0.0062598. Overall, Polynomial Regression is the most effective model for this data, while Random Forest and SVM also provide reliable predictions.

P-sensor: Similar to K-sensor, we have modified the P-sensor with a P-ISM layer to detect P concentrations in a test media. During testing, we introduced a number of dose-dependent phosphate concentrations and recorded the P-sensor's OCP. The open circuit potential of the P-sensor is inversely proportional to PO_4^{2-} concentrations. This behavior is attributed to the phosphate ion-selective membrane (P-ISM), which traps PO_4^{2-} ions from the testing solution, generating an interfacial potential that alters the overall OCP of the sensor (**Fig. 3A**). As tested, this P-sensor can detect a very low concentration of PO_4^{2-} ions, which is 200 ppt (parts-per-trillion) and can detect a higher concentration of 200 ppm, then it becomes saturation. The ability to detect 200 ppt of PO_4^{2-} ions is primarily attributed to the sensor's wrinkled surface structure. This P-sensor showed a moderate selectivity as evidenced by its low relative standard deviation of ± 7.8 (**Fig. 3C**). However, the selectivity of the P-sensor will be enhanced by an additional layer of tetradodecylammonium tetrakis (4-chlorophenyl) borate (ion exchange membrane or ETH 500),⁷ which permits only PO_4^{2-} ions during the ion exchange process.

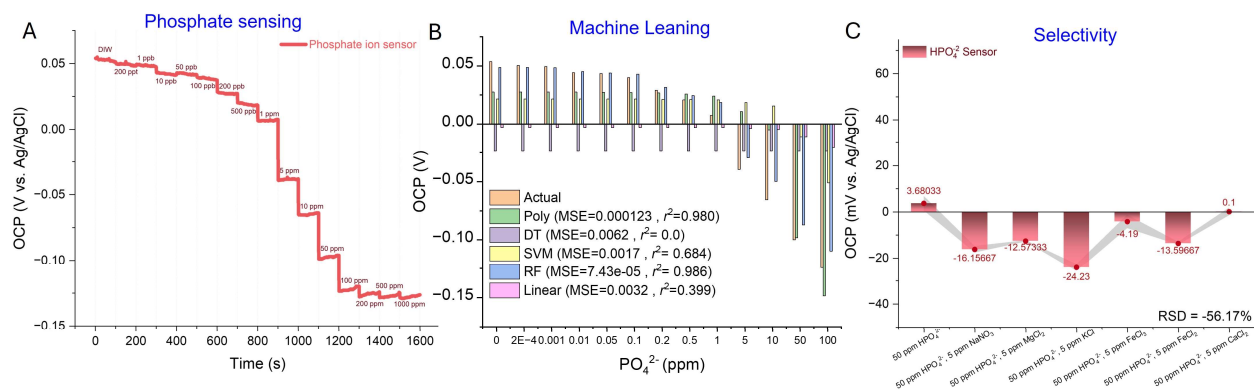


Figure 3. A) Calibration plot of the P-sensor, demonstrating its performance over a wide range of phosphate ion concentrations (200 ppt to 1000 ppm). B) Machine learning analysis using various regression models to determine the best fit for the calibration graph. C) Selectivity studies highlighting the P-sensor's response in the presence of common interfering ions.

The P-sensor results from applying machine learning algorithms to the P-sensor data reveal that the Random Forest Regression model performs the best, with an r^2 of 0.9863 and a very low MSE of 7.4378e-05, indicating it explains most of the variance and provides highly accurate predictions (**Fig. 3B**). Polynomial Regression also performs well with an r^2 of 0.8905 and a low MSE, suggesting a strong fit. The SVM model shows moderate performance with an r^2 of 0.6843 and MSE of 0.0017. In contrast, Linear Regression (r^2 : 0.3991, MSE: 0.0033) and DT regression (r^2 : 0, MSE: 0.0054) perform poorly, with the decision tree failing to capture any meaningful patterns. Overall, the RF model is the most accurate and suitable for predicting phosphate concentration based on sensor output.

N-sensor: For the N-sensor, we calibrated the device using dose-dependent nitrate concentrations in DI water (**Fig. 4A**). This N-sensor can detect a wide range of nitrate concentrations, from 1 ppm to 1200 ppm. The OCP of the N-sensor is inversely proportional to the nitrate concentration, with a sensitivity down to 1 ppm. The high selectivity of the N-sensor is attributed to the nitrate-selective membrane (**Fig. 4C**) in presence of interfering ions such as K^+ , Na^+ , and Cl^- . Likewise, P- and K-sensor, our N-sensor data was modeled using five different machine learning algorithms to evaluate the best fitting (**Fig. 4B**). The Random Forest model performed the best, with an r^2 of 0.87 and the lowest MSE of 0.00089, indicating strong predictive accuracy. The Polynomial Regression also performed well, achieving an r^2 of 0.79 and a moderate MSE of 0.0014. The SVM showed a moderate fit with an r^2 of 0.54 and MSE of 0.0031, while Linear Regression provided a decent fit with an r^2 of 0.64 and an MSE of 0.0024. The Decision Tree model, however, was the least effective, with an r^2 of 0 and a relatively high MSE of 0.0067, indicating poor performance for this dataset.

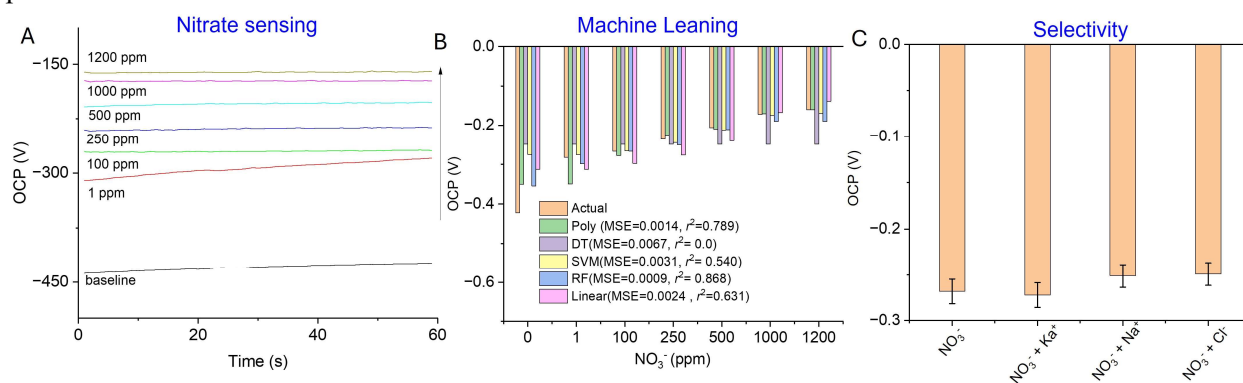


Figure 4. A) Calibration plot of the N-sensor, demonstrating its performance over a wide range of nitrate ion concentrations (1 ppm to 1200 ppm). B) Machine learning analysis using various regression models to determine the best fit for the calibration graph. C) Selectivity studies highlighting the N-sensor's response in the presence of common interfering ions.

Ongoing Greenhouse Experiments: Before deploying the sensors in real corn fields, we are conducting tests on greenhouse-grown corn plants to validate their performance. In our ongoing greenhouse experiments, we aim to evaluate the performance of the plant-implantable sensors by directly inserting them into the stalks of corn plants to monitor nutrient uptake. These experiments are being conducted at the Virginia Tech greenhouse facilities, where corn plants are grown under various soil conditions, including field soil without fertilizer, field soil amended with poultry litter, manure-enriched soil, and commercial potting soil. Once the corn plants reach the V9 growth stage, the needle-shaped sensors will be implanted into the stalks. Our plan is to monitor nutrient levels at each growth stage up to the V14 stage. These sensors will provide continuous, long-term monitoring of nitrogen (N), phosphorus (P), and potassium (K) uptake, allowing us to study the dynamic interactions between soil amendments and nutrient absorption in real-time.

Outcome and Conclusions. In summary, we successfully developed and calibrated plant-implantable sensors for monitoring N, P, and K nutrients in corn plants. Based on preliminary data obtained from these sensors, we have submitted a \$650K grant proposal to NIFA-USDA for federal funding. Additionally, we have filed a patent application through VT Intellectual Property, aiming to advance this innovation toward commercialization. If funded for the second year, we plan to validate the sensors through extensive corn field trials.

References

- 1 Ali, M. A. & Ataei Kachouei, M. Advancing Multi-Ion Sensing with Poly-Octylthiophene: 3D-Printed Milker-Implantable Microfluidic Device. *Advanced Science*, 2408314 (2024).
- 2 Ali, M. A., Kachouei, M. A., Parkulo, J., Fernandes, T. & Osorio, J. Attomolar Sensitive Milk Fever Sensor using Wrinkled 3D Printed Multiplex Sensing Structures. (2024).
- 3 Singh, A., Thakur, N. & Sharma, A. in *2016 3rd international conference on computing for sustainable global development (INDIACom)*. 1310-1315 (Ieee).
- 4 Ahmed, U. *et al.* Efficient water quality prediction using supervised machine learning. *Water* **11**, 2210 (2019).
- 5 Bhardwaj, R. *et al.* Modeling and simulation of temperature drift for ISFET-based pH sensor and its compensation through machine learning techniques. *International Journal of Circuit Theory and Applications* **47**, 954-970 (2019).
- 6 Crutchfield, J. D. & Grove, J. H. A new cadmium reduction device for the microplate determination of nitrate in water, soil, plant tissue, and physiological fluids. *Journal of AOAC International* **94**, 1896-1905 (2011).
- 7 Chen, Y., Liang, R. N. & Qin, W. Potentiometric sensor for sensitive and selective detection of heparin. *Chinese Chemical Letters* **23**, 233-236 (2012).